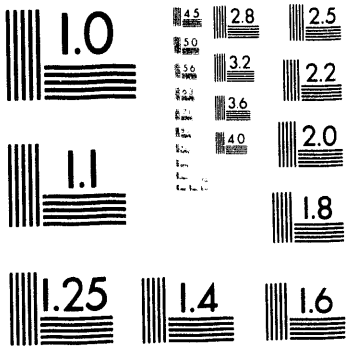
1.0
1.1
1.25
1.4
1.6
1.8
2.0
2.2
2.5
2.8
3.2
3.6
4.0
4.5
5.0
5.6

1 of 1

Abstract # : 314
Program # : EM-TuM4
Put on JVST manuscript

MBE GROWN III-V STRAIN RELAXED BUFFER LAYERS AND SUPERLATTICES CHARACTERIZED BY ATOMIC FORCE MICROSCOPY

A.J. Howard, I.J. Fritz, T.J. Drummond, J.A. Olsen,
B.E. Hammons, S.R. Kurtz and T.M. Brennan
Sandia National Laboratories, Albuquerque, NM 87185-5800

Abstract

Using atomic force microscopy (AFM), we have investigated the effects of growth temperature and dopant incorporation on the surface morphology of MBE grown graded buffer layers and strained layer superlattices (SLSs) in the InGaAlAs/GaAs and InAsSb/InSb material systems. Our AFM results show quantitatively that over the temperature range from 380 to 545 ^{o}C, graded $In_xAl_{1-x}As$ (x =0.05 - 0.32) buffer layers grown at high temperatures (~520 ^{o}C), and graded $In_xGa_{1-x}As$ (x =0.05 - 0.33) buffer layers and $In_{0.4}Ga_{0.6}As$ / $In_{0.26}Al_{0.35}Ga_{0.39}As$ SLSs grown at low temperatures (~400 ^{o}C) have the lowest RMS roughness. Also, for SLSs of $InAs_{0.21}Sb_{0.79}$/InSb, undoped layers grown at 470 ^{o}C were smoother than undoped layers grown at 420 ^{o}C and Be-doped layers grown at 470 ^{o}C. These results illustrate the role of surface tension in the growth of strained layer materials near the melting temperature of the $InAs_xSb_{1-x}$ /InSb superlattice. Nomarski interference and transmission electron microscopies, IR photoluminescence, x-ray diffraction, and photocurrent spectroscopy were also used to evaluate the relative quality of the material but usually, the results were not conclusive.

INTRODUCTION

Strained layer heterostructures are of interest for a wide variety of device applications due to their flexibility in electronic and optoelectronic properties which results from the wide range of compositions available, and strain-induced and quantum size effects[1,2]. Thick, high-quality semiconductor strained layer superlattices (SLSs)

can be grown as long as the individual layers are below the critical thickness and the multilayers are grown lattice matched to a relaxed buffer[3]. Devices such as 1.3 μm electro-optic modulators and 10 - 20 μm infra-red detectors, which have applications in optical communication and infrared detection applications, respectively, can be realized using the strained layer heteroepitaxy approach. Alloys of $In_xGa_{1-x}As$ and $In_xAl_{1-x}As$ and strained layer superlattices (SLSs) of $InAs_xSb_{1-x}$ / InSb have the proper lattice constants and/or band gaps for these applications, but epitaxial growth of these materials is difficult due to the lack of suitable lattice-matched substrates. By combining SLSs with graded relaxed buffer layers, both 1.3 μm modulators[4] and IR detectors[5] have been fabricated on GaAs and InSb substrates, respectively.

Successful fabrication of these strained layer devices is contingent upon optimizing the placement and density of dislocations. Misfit dislocations, which form when the critical layer thickness is exceeded, provide for strain accommodation [3]. Threading dislocations in the growth direction, however, limit epi-layer quality and degrade device performance. In addition to dislocations, micro-cracks and cross-hatching can be observed when growing strained layer structures. Until recently, a characterization tool which can quantitatively assess the quality of strained layer surfaces on the appropriate length scale, did not exist, and this made structural optimization extremely difficult. The AFM, which operates in air, without sample preparation, is non-destructive, and is easy to use, fills this characterization void.

Reports on the effects of layer design and growth conditions on material quality in graded buffer layers and SLSs exist, but the results are confusing and contradictory[6-10]. We have studied the effects of growth temperature and doping on the quality of the SLSs and graded buffer layers in the InGaAlAs/GaAs and InAsSb/InSb material systems as part of 1.3 μm modulator and IR detector development programs. The surface morphology of the MBE grown material has been characterized in detail by AFM. Nomarski phase contrast microscopy, transmission electron microscopy (TEM),

photocurrent spectroscopy (PCS), and IR photoluminescence were also performed and the results will be presented in this paper.

EXPERIMENTAL

All of the GaAs based structures for this study were grown in a RIBER 32P MBE system. The growth rates were calibrated using reflection high energy electron diffraction and the substrate temperatures were monitored using an Ircon infrared pyrometer. Epi-ready, (100) n^+-GaAs substrates were used and mounted using an indium-free holder. As_2 was used at a V/III ratio of ~ 9. Silicon and beryllium were the n- and p-type dopants, respectively. The growth rates were 3.12, 0.78 and 1.92 Å/sec for GaAs, AlAs and InAs, respectively, and were reproducible to within ±0.5%.

The goal of this materials study was the production of a high quality relaxed buffer layer (with a planar lattice constant larger than that of GaAs) and SLS structure which would be suitable for the active region of a 1.3 μm modulator. The design considerations and test results of the completed device are presented elsewhere[4]. Two separate structural approaches were taken. SLSs of 83 Å $In_{0.4}Ga_{0.6}As$ / 80 Å $In_{0.26}Al_{0.35}Ga_{0.39}As$ were grown on linearly graded buffer layers of either $In_xGa_{1-x}As$ (x=0.05 - 0.33) or $In_xAl_{1-x}As$ (x=0.05 - 0.32). We decided to vary the growth temperature profile in our buffer/SLS structure. The generic test structure for these experiments in shown schematically in Fig. 1. T_B and T_{SLS} stand for the buffer layer and SLS/cap layer growth temperatures, respectively. For the InGaAs buffer approach, samples with the combined InGaAs buffer and SLS were grown at T_B/T_{SLS} of 540/540, 400/540 and 400/400 C. For the InAlAs buffer approach, samples with just the buffer layer were grown at T_B of 520, 470, and 420 C. Then, samples with both the InAlAs buffer and SLS were grown at T_B/T_{SLS} of 470/545, 470/470, 470/420 and 470/380 C. Whenever it was necessary to change the growth temperature from T_B to T_{SLS}, this was achieved via ramping during the constant composition buffer layer (Buffer 2) growth. The effects of growth temperature on surface morphology were characterized

by AFM. All AFM micrographs were taken using a Digital Instruments Nanoscope III atomic force microscope operating in air in contact mode. Other characterization techniques such as Nomarski interference, TEM, and PCS were also performed.

The InSb based materials were grown in a Vacuum Generators VH 80 MBE system. Micro-crack suppression in step-graded $Ga_xIn_{1-x}Sb$ (x=0.00 - 0.14) buffer layers grown on InSb has been previously optimized, and the details of the buffer growth are discussed elsewhere[11]. In this study, our goal was the optimization of the surface morphology and optical quality of $InAs_{0.21}Sb_{0.79}$ /InSb SLSs grown on step-graded $Ga_xIn_{1-x}Sb$ buffers on InSb substrates for infrared detector applications. The generic test structure for the InSb-based experiments is shown schematically in Fig. 2. The buffer was a five layer structure going from InSb to $Ga_{0.14}In_{0.86}Sb$ in equal 2.8% Ga steps. The growth rate was maintained at 1 μm/hr using a constant Sb/In atomic flux ratio of 2; the V/III ratio was higher during the growth of alloys due to the addition of As_2 which was thermally cracked from As_4. The Be flux was set to yield a doping level of $p \sim 8 \times 10^{17}$ cm^{-3} in the 1.0 μm thick pre-buffer and the five ~0.4 μm thick buffer layers. The pre-buffer and graded buffer layers were grown at 470 °C on a (100) p^+-InSb substrate which was coated on the backside with 200 nm of WC (In solder barrier) and 50 nm of Au (wetting agent). In order to achieve optical absorption at a wavelength slightly longer than 10 μm, equal layer thicknesses of nominally 99 Å of $InAs_{0.21}Sb_{0.79}$ and InSb were grown. The unintentionally doped 2 μm thick SLSs were grown at temperatures of 470 and 420 °C. The Be-doped ($p=5 \times 10^{15}$ cm^{-3}) 1 μm thick SLS was grown at 470 °C. The effects of growth temperature and Be-doping on SLS material quality were characterized by Nomarski phase contrast and atomic force microscopies and IR photoluminescence.

RESULTS AND DISCUSSION

A 1.3 μm reflectance modulator was successfully fabricated using the InGaAs graded buffer layer approach[4]. Understanding the effects of different growth

temperatures on the quality of the combined buffer and SLS structure (see Fig. 1) was a key element in our success[12]. As was stated previously, numerous test structures of InAlAs graded buffers alone and also combined InAlAs buffer/SLS and InGaAs buffer/SLS were grown at various T_B and T_{SLS} combinations over the temperature range of 380 to 545 ^oC. X-ray diffraction was performed on the samples and the measurements showed the buffers to be near full relaxation. All of the samples exhibited either a slightly cross-hatched or specular surface when viewed by Nomarski phase contrast microscopy; some of the samples had slightly smoother surfaces, but this observation was not quantifiable. Cross-sectional TEM was also performed and a typical micrograph is shown in Fig. 3. All of the TEM micrographs showed the same low density ($<10^6$ cm^{-2}) of dislocations in the 0.2 μm thick constant-composition buffer and, if present, SLS regions. Many strain-relieving misfit dislocations were observed in the 2.5 μm thick graded InGaAs or InAlAs buffer.

After unsuccessfully trying to quantify the relative quality of the test structures using X-ray diffraction, Nomarski phase contrast microscopy and TEM, atomic force microscopy was then employed. Using the Digital Instruments system, which has a built-in software package for the analysis of RMS surface roughness and for the deviation of the surface area from perfect planarity, $\Delta A/A$, AFM images of the surfaces were taken and analyzed for all of the test structures. A summary of the average (data was taken at 5 to 10 points on the two inch wafers) RMS roughness and $\Delta A/A$ data are given in Table I. Finally, it was possible to assess the quality of the test structures grown at different conditions! For the InAlAs buffers alone, it is clear that the higher T_B values (470 to 520 ^oC) result in smoother surfaces. AFM images of the two extremes in T_B investigated for InAlAs buffers are shown in Fig. 4; everything except T_B was the same during the growth of these samples. The T_B=420 ^oC sample has a fine scale, spiky appearance which is consistent with the large RMS roughness (14.1 nm) for the sample, whereas the 520 ^oC sample is much smoother (RMS=2.6 nm).

For the combined InAlAs buffer/SLS structure study, all of the samples were grown using T_B=470 ^oC. This decision was based on the results from the InAlAs buffer study. The AFM characterization results for these samples are also presented in Table I. AFM images of all four of the samples had similar cross-hatched surface morphologies. This probably occurred because the InAlAs graded buffer growth was already independently optimized. The outcome from this study was not as staggering as the results from the InAlAs buffer study, but it did point us in the direction that the SLS should be grown at the lower end (T_{SLS}=380 to 420 ^oC) of the temperature range investigated. Consequently, a full 1.3 μm transmission modulator structure was grown and functioning devices were recently fabricated using the InAlAs graded buffer on GaAs approach. The device structure was grown using the T_B/T_{SLS}=470/420 ^oC condition; test results for these devices will be published elsewhere[13].

Table I also includes the results from the combined InGaAs buffer/SLS structure study. There is a significant difference in the RMS surface roughness (13.9 to 5.7 nm) for these samples. AFM images of the samples with the two extremes in roughness, T_B/T_{SLS}=400/400 and 540/540 ^oC, are presented in Fig. 5. Clearly, the AFM images and data show that the InGaAs buffer/SLS structure should be grown at the lower end of the temperature range (~400 ^oC) investigated. Having completed this optimization, 1.3 μm reflectance modulators were fabricated using the InGaAs buffer/SLS T_B/T_{SLS}=400/400 ^oC growth condition. The reflectance modulators operate at 1.33 μm with a ~4 dB insertion loss, a maximum $\Delta R/R$ of 68 % and a contrast ratio of 2.7:1 at a bias of 4 volts. More details on the device design and test results are given elsewhere[4].

The combined buffer/SLS test structures (see Fig. 1) were doped to form a p-i-n detector. This allowed us to assess the optical quality of the structures by performing PCS. This characterization technique was performed on the InGaAs buffer/SLS and InAlAs buffer/SLS samples. The results for InGaAs buffer/SLS samples are plotted in

Fig. 6. The three structures displayed excitonic absorption at 1.28, 1.28 and 1.30 μm, but the widths of the excitons are different. The T_B/T_{SLS}=400/400 ^oC structure has the narrowest excitonic features with the exciton located closest to the design goal of 1.30 μm. This result is in agreement with our AFM results. All of these structures were grown sequentially at fixed growth rates, hence long-term drifts in the group III sources are unlikely to cause excitonic broadening. We believe the broadening is due to lateral strain and/or compocitional non-uniformities due to surface texturing[14]. The slight shift to ~ 1.28 μm for the T_B/T_{SLS}=400/540 ^oC and 540/540 ^oC samples can be explained by increased surface segregation of indium at the higher growth temperatures, which decreases indium incorporation and widens the bandgap[15]. PCS was also performed on the InAlAs buffer/SLS structures. The results were similar to the PCS-AFM results correlation observed for the InGaAs buffer/SLS structures: samples with superior (narrow excitons) optical quality have superior (smoother) surface morphologies.

For the InAsSb/InSb SLSs, as evaluated by Nomarski phase contrast microscopy, smooth cross-hatched SLS surface morphologies are obtained only at very high growth temperatures as compared to homoepitaxial InSb. High quality InSb is obtained for growth temperatures close to 420 °C while the growth temperature required to obtain smooth SLSs (at 1 μm/hr and Sb/In = 2.0) was 470 °C. This is in excess of 90% of the melting temperature of InSb. At the growth temperature of 470 °C the addition of Be at doping levels as low as 5 $x10^{15}$ cm^{-3} were found to degrade the surface morphology more severely than low growth temperatures. The optical response of the superlattices correlated with the surface morphology. Only the undoped SLS with a smooth cross-hatched surface showed any optical response at all. The photoluminescence and photoconductivity response of a smooth high temperature SLS are shown in Figure 7. This sample displayed intense luminescence at 14 K with a linewidth of 9 meV, one of the narrowest lines ever observed in this type II superlattice system.

To quantify the Nomarski results AFM was employed to further characterize the surface morphology of the superlattices. The results are summarized in Table I. As expected, the RMS roughness and $\Delta A/A$ values are smaller for the undoped samples than for the Be doped sample. The AFM image for the doped and undoped samples grown at 470 ^{o}C are shown in Figure 8. Although we cannot, as yet, rule out dopant precipitation as a cause for the poor morphology of the doped SLS, a comprehensive explanation can be made using surface tension as the relevant process variable. In the undoped superlattices the alternating layers are elastically soft and subject to alternating tensile and compressive stresses. The InSb layers under compressive stress will facet if the surface tension is low and the interlayer strain is sufficiently high. Increasing the substrate temperature under a fixed V/III ratio will increase the Sb desorbtion rate making the surface increasingly metal rich and thereby increase the surface tension which will act to suppress faceting. This explanation is consistent with other results obtained at higher and lower interlayer strains. In the case of the doped layer it is know that Be strongly surface segregates during the growth of homoepitaxial InSb grown at much lower temperatures. At a temperature of 470 ^{o}C it is proposed that virtually all of the Be surface segregates thereby modifying the surface tension (or promoting precipitation) as the Be surface concentration approaches a critical fraction of a monolayer. Assuming that surface Be lowers the surface tension, faceting of the InSb layers will once again be favorable. The accumulation of surface Be is expected to be self limiting as facets which are rich in cation sites will be favored by being more effective at incorporating Be. A more complete exposition of this model will be presented elsewhere [16].

CONCLUSIONS

Using AFM we have investigated the effects of growth temperature and dopant incorporation on the surface morphology of MBE grown graded buffer layers and strained layer superlattices (SLSs) in the InGaAlAs/GaAs and InAsSb/InSb material

systems. Our AFM results, which are in agreement with PCS results, show quantitatively that over the temperature range 380 - 545 ^{o}C, linearly graded $In_xAl_{1-x}As$ (x =0.05 - 0.32) buffer layers grown at high temperatures (~520 ^{o}C) and linearly graded $In_xGa_{1-x}As$ (x =0.05 - 0.33) buffer layers and $In_{0.4}Ga_{0.6}As$ / $In_{0.26}Al_{0.35}Ga_{0.39}As$ SLSs grown at low temperatures (~400 ^{o}C) have the lowest RMS roughness and superior optical quality. For SLSs of $InAs_{0.21}Sb_{0.79}$/InSb grown on relaxed, step-graded GaInSb buffer layers on InSb, undoped SLSs grown at 470 ^{o}C were smoother than undoped layers grown at 420 ^{o}C and Be-doped layers grown at 470 ^{o}C. We propose that Be surface segregation decreases the (100) InSb growth surface tension which leads to faceting and rougher surfaces. Surface tension is a key contributing factor in the growth of strained layer materials near the melting temperature of the $InAs_xSb_{1-x}$ /InSb superlattice. Other characterization techniques such as Nomarski interference and transmission electron microscopies, IR photoluminescence, x-ray diffraction, and photocurrent spectroscopy were also used to evaluate the materials. The AFM, however, provides valuable quantitative and morphological information which was not available using these other techniques.

ACKNOWLEDGMENTS

The authors would like to thank Dr. L.R. Dawson for the use of his MBE system and Mark Rodgers and Kevin Kjoller of Digital Instruments, Inc. of Santa Barbara, CA for their assistance with the AFM. We would also like to thank R. Hibray, L. Griego, J. Bur and J.M. Sergeant for their expert technical assistance. This work was supported by the U.S. Dept. of Energy under Contract DE-AC04-~~76DP00789~~.
94 AL 85000

REFERENCES

[1] G.C. Osburn, J. Vac. Sci. Technol. **B1**, 379 (1983).

[2] P.L. Gourley and R.M. Biefeld, J. Vac. Sci. Technol. **B1**, 383 (1983).

[3] J.W. Matthews and A.E. Blakeslee, J. Cryst. Growth **32**, 265 (1976).

[4] I.J. Fritz, B.E. Hammons, A.J. Howard, T.M. Brennan and J.A. Olsen, Appl. Phys. Lett. 62, 919 (1993).

[5] S.R. Kurtz, L.R. Dawson, T.E. Zipperian and R.D. Whaley, Jr., IEEE Elect. Dev. Lett. **11**, 54 (1990).

[6] E.A. Fitzgerald, Y.H. Xie, D. Monroe, P.J. Silverman, J.M. Kuo, A.R. Kortan, F.A. Thiel and B.E. Weir, J. Vac. Sci. Technol. B **10**, 1807 (1992).

[7] J.C.P. Chang, J. Chen, J.M. Fernandez, H.H. Weider and K.L. Kavanagh, Appl. Phys. Lett. **60**, 1129 (1992).

[8] J.C. Harmand, T. Matsuno and K. Inoue, Jap. Jour. Appl. Phys. **28**, L1101 (1989).

[9] P. Ribas, V. Krishnamoorthy and R.M. Park, Appl. Phys. Lett. **57**, 1040 (1990).

[10] S.M. Lord, B. Pezeshki and J.S. Harris, Jr., Elect. Lett. **28**, 1193 (1992).

[11] T.J. Drummond and S.R. Lee, Presented at Mat. Res. Soc. Symp. P, Spring (1993) and to be published elsewhere.

[12] B.E. Hammons, I.J. Fritz, T.M. Brennan, A.J. Howard and J.A. Olsen, J. Vac. Sci. Technol. B, 932 (1993).

[13] I.J. Fritz, A.J. Howard, B.E. Hammons, J.A. Olsen and T.M. Brennan, To be submitted.

[14] T.K. Woodward, T. Sizer, II, D.L. Sivco and A.Y. Cho, Appl. Phys. Lett. **57**, 548 (1990).

[15] K. Muraki, S. Fukatsu, Y. Shiraki and R. Ito, Appl. Phys. Lett. **61**, 557 (1992).

[16] T.J. Drummond, S.R. Kurtz and S.R. Lee, Presented at Mat. Res. Soc. Symp. C, Spring (1993) and to be published elsewhere.

DISCLAIMER

FIGURE CAPTIONS

Figure 1. Structure used for the InAlAs buffer alone and combined InAlAs buffer /SLS and InGaAs buffer/SLS test samples.

Figure 2. Structure used for the InAsSb/InSb SLS undoped and Be-doped test samples. The Be-doped SLS sample was only 1 μm thick.

Figure 3. Cross-sectional TEM micrograph of a InGaAs buffer/SLS structure. Essentially all of the dislocations are located in the linearly graded buffer layer.

Figure 4. AFM images of InAlAs buffer samples (without SLSs) grown at (a) 520 ^{o}C (smoothest) and (b) 420 ^{o}C (roughest).

Figure 5. AFM images of InGaAs buffer/SLS samples grown at T_B/T_{SLS}= (a) 400/400 ^{o}C (smoothest) and (b) 540/540 ^{o}C (roughest).

Figure 6. Photocurrent spectra of the InGaAs buffer/SLS samples grown at different T_B/T_{SLS}. The 400/400 ^{o}C sample has the narrowest and sharpest excitonic features.

Figure 7. PL and PC spectra for the best undoped InAsSb/InSb SLS. The sample was grown at T_{SLS}=470 ^{o}C. The PL linewidth is among the narrowest (9 meV) reported for this material system.

Figure 8. AFM images of the (a) undoped and (b) Be-doped InAsSb/InSb SLSs both grown at T_{SLS}=470 ^{o}C. The Be-doped SLS surface is faceted due to Be segregation.

Table I

AFM statistics and growth conditions for buffer layers and SLSs grown on GaAs and InSb. The first series of InAlAs/GaAs samples were grown without SLSs. The "470-Be" sample had an intentionally Be-doped SLS, all other SLSs were undoped.

Buffer Material/Substrate	T_B(/T_{SLS}) (^oC)	RMS Roughness (nm)	$\Delta A/A$ (%)
InAlAs/GaAs	520	2.6	0.007
	470	2.8	0.052
	420	14.1	6.797
InAlAs/GaAs	470/545	8.4	0.011
	470/470	8.6	0.016
	470/420	6.9	0.016
	470/380	6.0	0.008
InGaAs/GaAs	540/540	13.9	0.229
	400/540	10.1	0.060
	400/400	5.7	0.108
GaInSb/InSb	470/420	5.1	0.008
	470/470	3.3	0.001
	470/470-Be	7.4	0.014

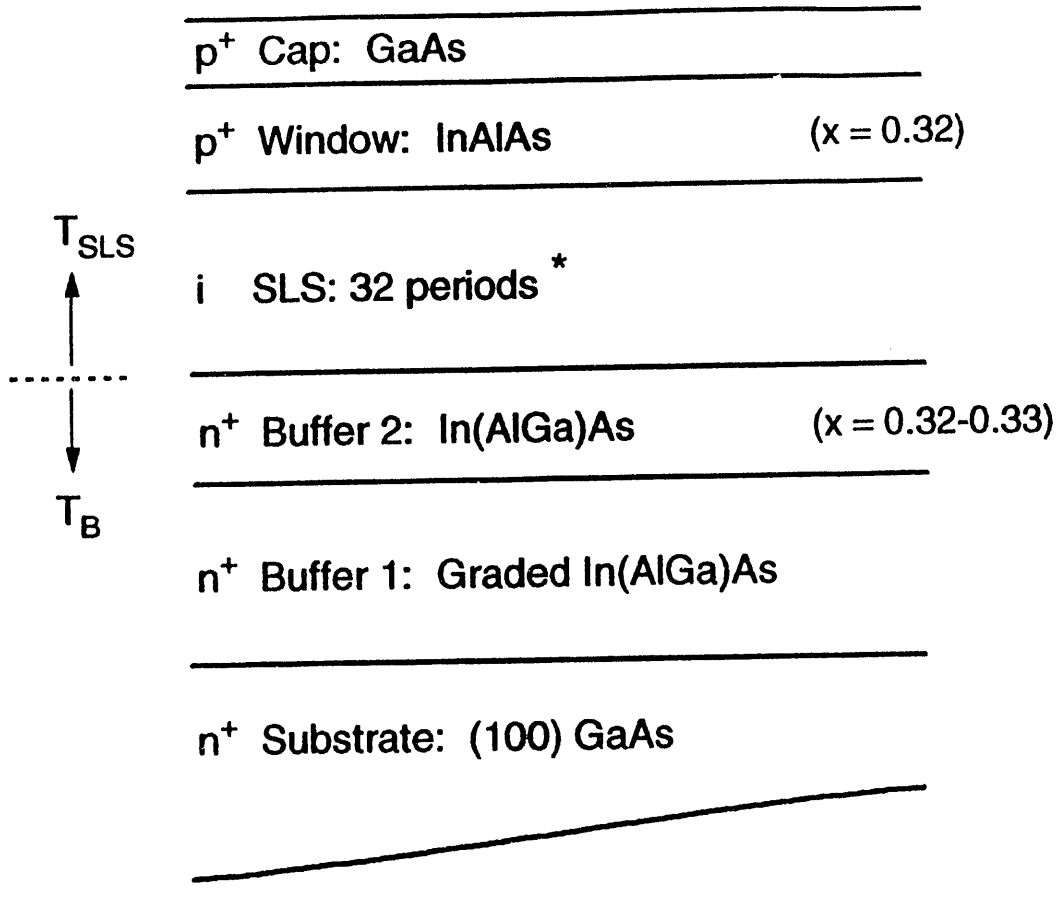

* SLS: $In_{0.4}Ga_{0.6}As/In_{0.26}Al_{0.35}Ga_{0.39}As$
8.2/8.2 nm

Fig. 1

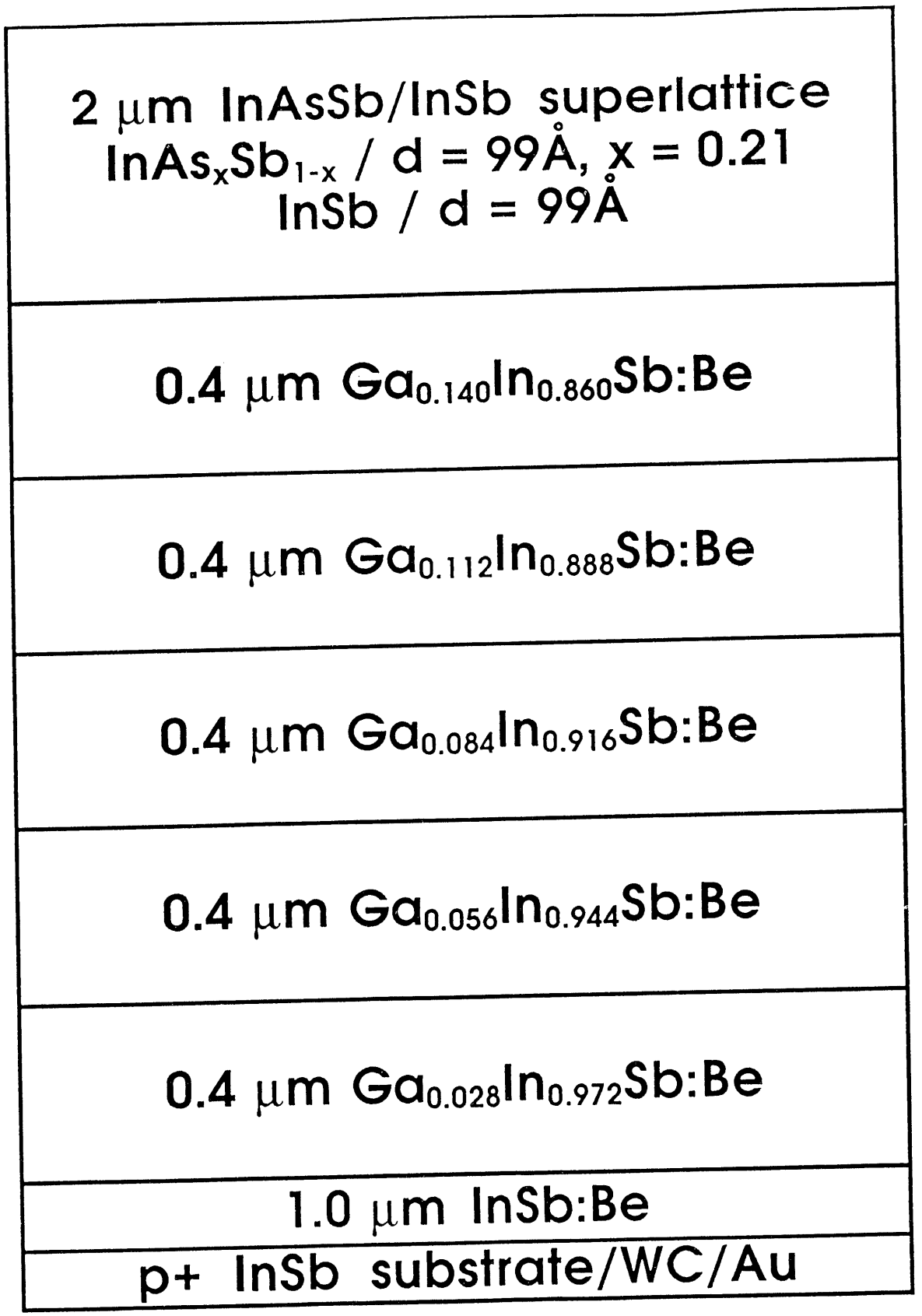
2 μm InAsSb/InSb superlattice
InAsxSb1-x / d = 99Å, x = 0.21
InSb / d = 99Å
0.4 μm Ga0.140In0.860Sb:Be
0.4 μm Ga0.112In0.888Sb:Be
0.4 μm Ga0.084In0.916Sb:Be
0.4 μm Ga0.056In0.944Sb:Be
0.4 μm Ga0.028In0.972Sb:Be
1.0 μm InSb:Be
p+ InSb substrate/WC/Au

Fig. 2

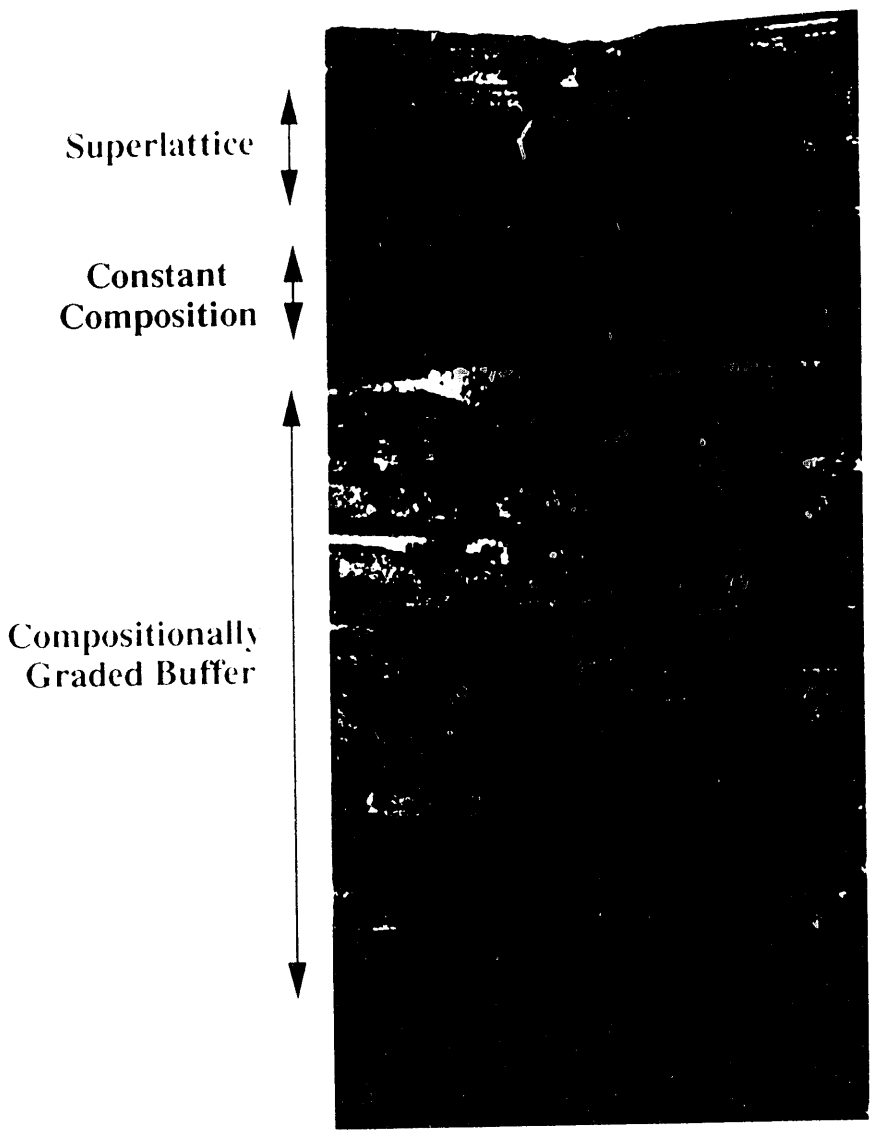
Superlattice
Constant Composition
Compositionally Graded Buffer

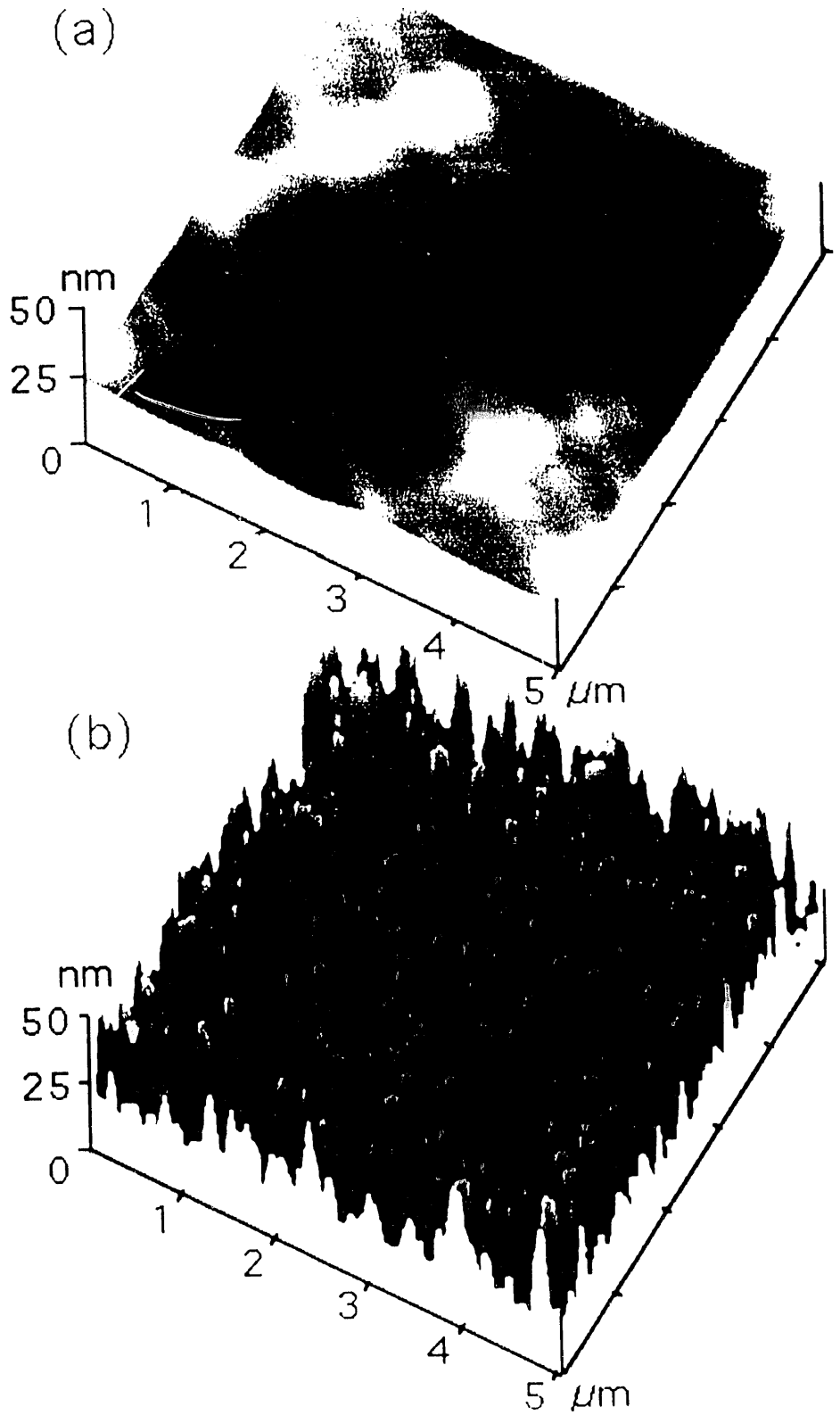
(a)
nm
50
25
0
1
2
3
4
5 μm
(b)
nm
50
25
0
1
2
3
4
5 μm

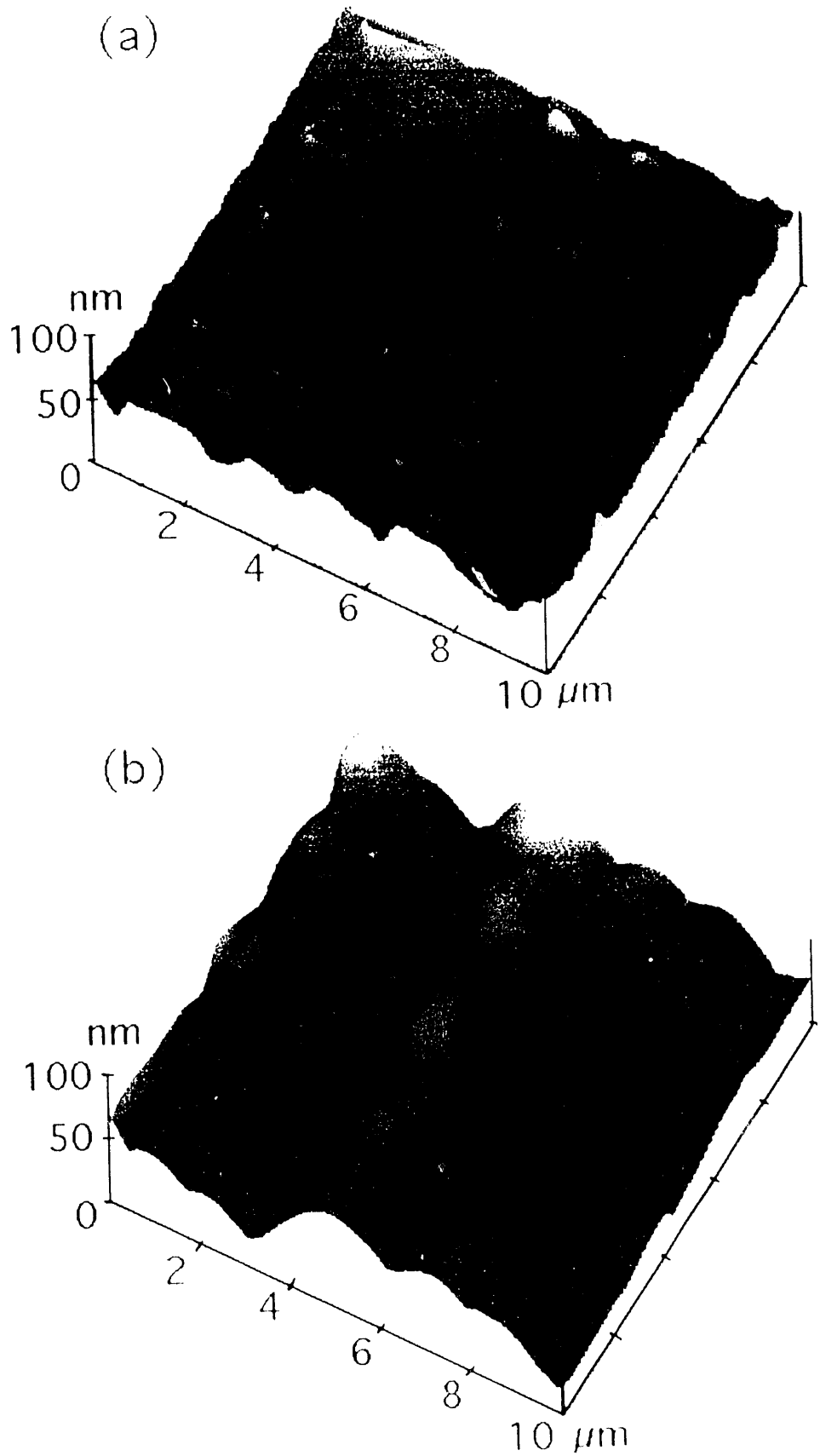
(a)
nm
100
50
0
2
4
6
8
10 μm
(b)
nm
100
50
0
2
4
6
8
10 μm

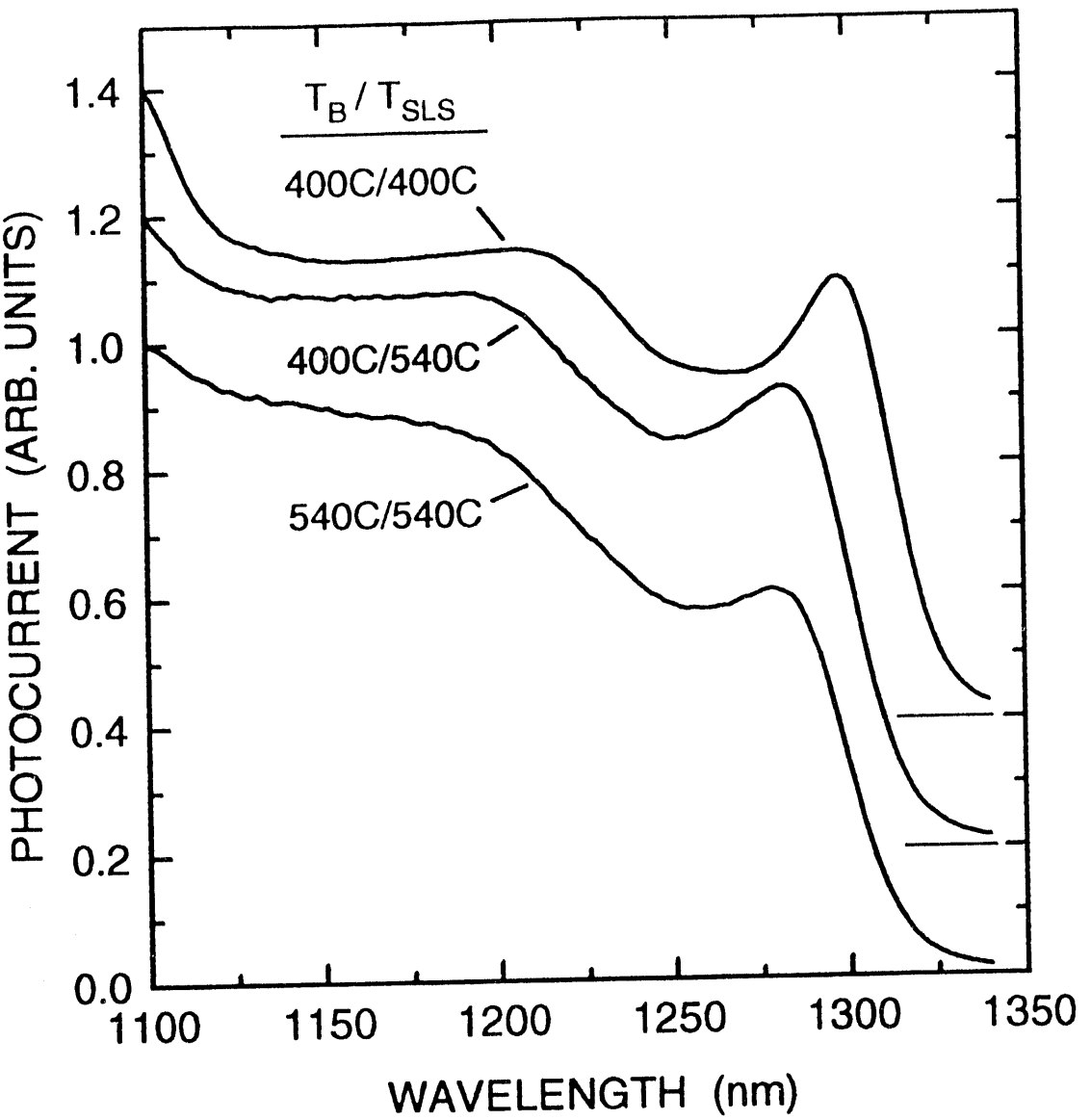
T_B / T_{SLS}
400C/400C
400C/540C
540C/540C
PHOTOCURRENT (ARB. UNITS)
1.4
1.2
1.0
0.8
0.6
0.4
0.2
0.0
1100
1150
1200
1250
1300
1350
WAVELENGTH (nm)

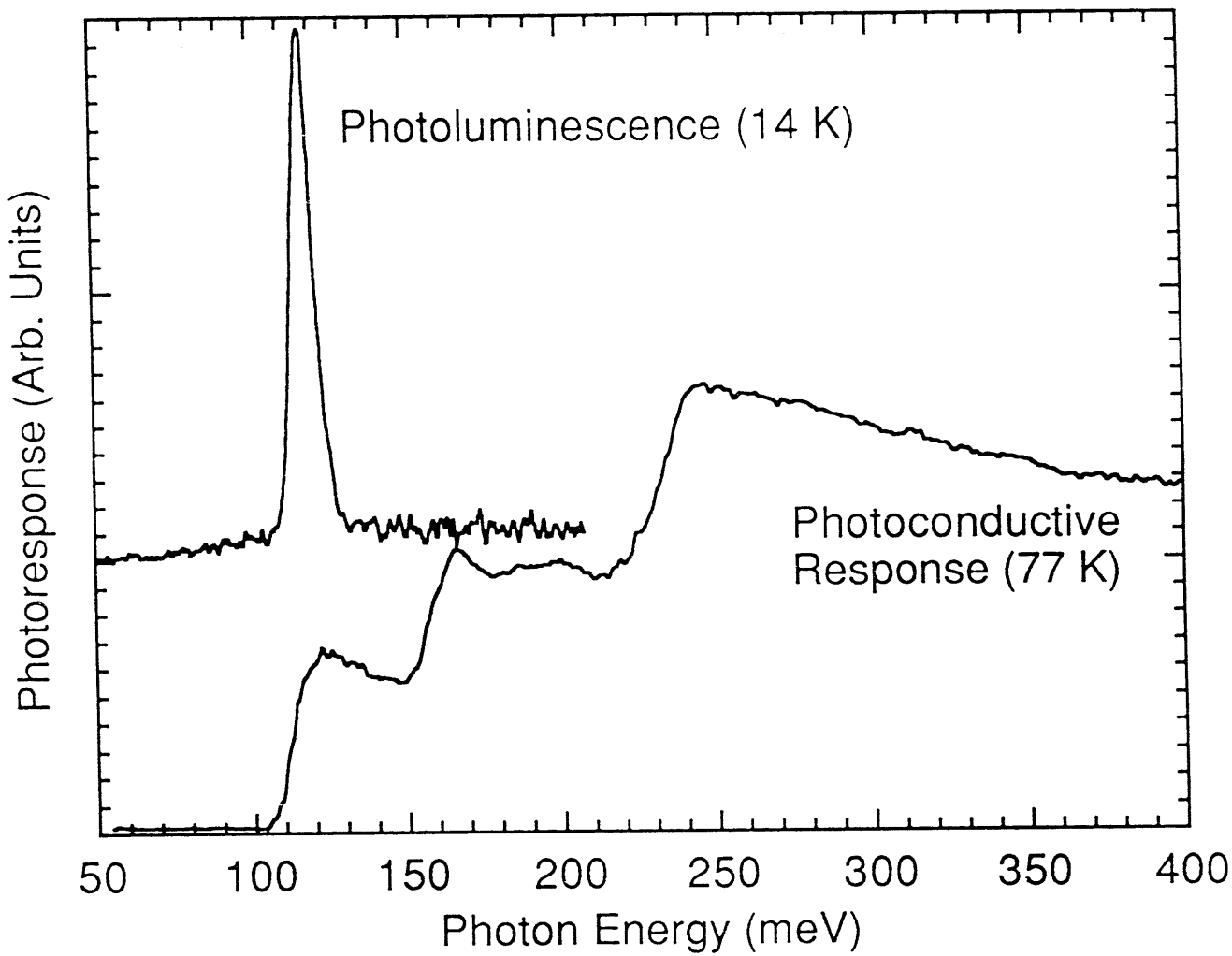
Photoluminescence (14 K)
Photoconductive
Response (77 K)
Photoresponse (Arb. Units)
50
100
150
200
250
300
350
400
Photon Energy (meV)

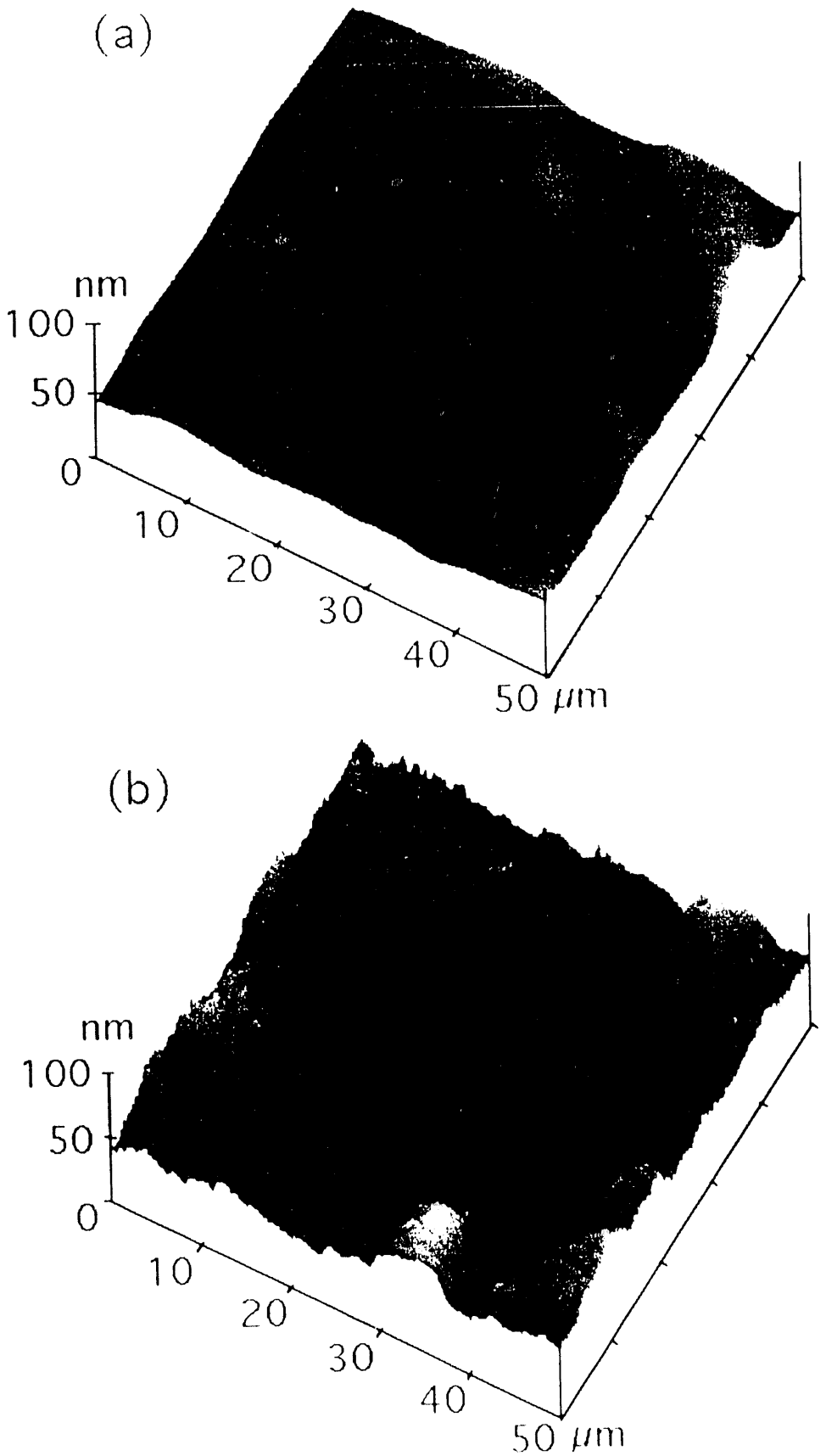
(a)
nm
100
50
0
10
20
30
40
50 μm
(b)
nm
100
50
0
10
20
30
40
50 μm

DATE FILMED

1 / 5 / 94

END